

NEM and MFEM Simulation of Interaction between Time-dependent Waves and Obstacles

V A Perminov¹, T S Rein², S N Karabtcev²

¹Tomsk national research polytechnic university, chair of ecology and health and safety, Tomsk, Russia

²Kemerovo state university, UNESCO NIT chair, Kemerovo, Russia

E-mail: p_valer@mail.ru, tsrein@mail.ru, skarab@kemsu.ru

Abstract. Fundamental research challenge of structural integrity and construction resistance while interacting with fluid or gas is of high importance when estimating their efficiency and lifetime. The paper presents the simulation results of interaction between incompressible ideal fluid and an escarpment at the bottom, and interaction between viscous incompressible fluid and an obstacle above fluid surface. Flow patterns at different times and chronograms of hydrodynamic loads on solid walls of computational domain, horizontal and vertical obstacles are displayed.

1. Introduction

The paper shows solution results of the problems dedicated to fluid interacting with vertical and horizontal obstacles in the context of classical nonlinear problem statement where velocity vector component and pressure domain are unknown. This statement enables to carry out comprehensive study of wave flows during all stages of simulation experiment including wave collapsing, vortex formation, turbulent flows with possible intermixing fluid layers formation.

Nowadays there is a whole range of mesh methods. Finite elements method (FEM) [1] and control volume method (CVM) [2] are the most popular of them. However, mesh-free methods [3] are more often used. They approximate equations into partial derivatives being based on nodes set without knowing any additional information about mesh structure. Smoothed Particle method [4], Lagrangian and Eulerian particles method [5] appear to be very efficient in the context of hydrodynamics and gasdynamics dynamics problems. Relatively low accuracy and difficulties based on carrying in boundary conditions are disadvantageous features of mesh-free methods.

The facts described above conducted to new conventionally mesh-free methods which include both ideas and opportunities of mesh-free methods and grid method advantages. Mesh-free finite elements method (MFEM) and natural element method [6, 7] appeared to be the first of new generation mesh-free methods.

Their main feature is that they occur to be usual (classical) Galerkin methods in the context of non time-dependent problems. To solve time-dependent problems Lagrange approach of medium description is applied: based on every time step a mesh is created, it identifies new structure of neighbors for each node of the domain. Equation system is solved again with the help of Galerkin method on newly-created grid. Thus, NEM and MFEM have some advantages of classical Galerkin method, that are simplicity of shape function in definition domain, continuity between elements, easy boundary conditions input. On the other hand they have all advantages of mesh-free methods, which means that natural element method form functions depend on node location.



2. Problem statement

Complete nonlinear problem of ideal incompressible fluid with free boundary is stated below.

Ideal incompressible fluid flow described by Euler equation system and equation of continuity is specified in flow D computational domain represented by finite node set and limited by free surface Γ_0 and solid boundaries Γ_1 , Γ_2 and Γ_3 :

$$\frac{Du_i}{Dt} = -\frac{1}{\rho} \frac{\partial p}{\partial x_i} + f_i, \mathbf{x} \in D, i = \overline{1,2}. \quad (1)$$

$$\partial u_i / \partial x_i = 0, \mathbf{x} \in D \quad (2)$$

Here $\mathbf{x} = (x_1, x_2)$ – spatial coordinates, $\mathbf{u} = (u_1, u_2)$ – velocity vector, p – pressure, ρ – density, $\mathbf{f} = (f_1, f_2) = (0, -g)$ – external force vector. Node motion in the domain is describe by the following equation:

$$dx_i / dt = u_i, \mathbf{x} \in D, i = \overline{1,2}. \quad (3)$$

Dynamic condition $p = p_{atm}$ is fulfilled on free surface Γ_0 , impermeability condition $\mathbf{u} \cdot \mathbf{n} = 0$ is fulfilled on solid boundaries Γ_1 , Γ_2 , Γ_3 , where $\mathbf{n} = (n_1, n_2)$ – the external normal to the fluid boundary.

General formulation of viscous incompressible fluid flow problem is presented below. Newtonian viscous incompressible fluid flow described by Navier-Stokes equations and equation of continuity (2) is considered to occur in flow domain D. Navier-Stokes equations are presented in Euler's formulation as follows:

$$\frac{Du_i}{Dt} = -\frac{1}{\rho} \frac{\partial p}{\partial x_i} + \frac{\mu}{\rho} \frac{\partial}{\partial x_j} \left(\frac{\partial u_i}{\partial x_j} \right) + f_i, i = \overline{1,2}, j = \overline{1,2}. \quad (4)$$

Pressure p and velocity vector \mathbf{u} are the required functions in equation system (2),(4). Density ρ , external forces vector \bar{f} and dynamic viscosity coefficient μ are the required parameters in equation system (2),(4).

Boundary conditions for Navier-Stokes equations (2),(4) are as follows: as far as fluid is viscous, no-slip boundary condition $u_i = 0, i = \overline{1,2}$ is fulfilled on solid boundaries Γ_1 , Γ_2 and Γ_3 . Dynamic condition $p = p_{atm}$ is fulfilled on free surface Γ_0 like in ideal fluid case.

It is needed to set nodes location $\mathbf{x}(0) = \mathbf{x}^0$ and distribution of unknown functions in whole flow domain $\mathbf{u}(\mathbf{x}, 0) = \mathbf{u}^0(\mathbf{x})$, $p(\mathbf{x}, 0) = p^0(\mathbf{x})$ for time-dependent problem of both viscous and ideal fluids flows.

3. Numerical computation

3.1. Mesh-free finite elements method

In 1994 L.Traversoni suggested natural elements [8] method should be used to solve plasticity theory problems. This method is a variation of Galerkin mesh-free method. Like Galerkin's method unknown functions are approximated as follows: $q = N^T Q$, where $q = (u_i, p, \rho)$, $i = \overline{1,2}$, Q – nodal values of unknown function, N - interpolating form function. Later the method was adapted to solve fluid flow problems and became more popular as mesh-free finite elements method [9].

Integrated form of weighted residuals method is used to create discrete equations system. Integrals taken are based on elements of extended Delone triangulation. Multitude of natural elements for each node and free boundary nodes at new time step are defined with the help of «sweep line» method и «alpha-shape» method respectively [10].

The essential difference of classical finite elements method from mesh-free method includes the necessity of computational mesh recreating at every time step. Each time new Sibson and Laplace interpolating functions [11,12] are constructed and rigidity matrixes are calculated, resulting equations are set up on a newly created mesh. Solution of multidimensional problem at fractional steps results in solution of individual equations with the help of conjugate gradient method.

To define the structure of neighbors and its nodes and to calculate Sibson and Laplace form functions the domain is divided by Voronoi cells [12]. Computational mesh is needed for numerical integration while calculating the elements of rigidity matrix of resulting equations (weak form of medium motion equation is under consideration).

At first time step the domain is divided with the help of Delone triangulation. Though, there is a necessity of computational mesh quality improvement in time-dependent problems (as soon as the mesh does not meet Delone criteria). If a mesh node location changes it is necessary to interpolate the variables values from the old “bad” mesh to the new upgraded one. Sibson and Laplace form functions are considered to be interpolation coefficients while recalculating the variables values.

3.2. Sibson and Laplace Interpolating functions

Focused on natural elements concept Sibson’s interpolating functions are based on Voronoi diagrams of the first and second order and identified by polygons area ratio in two-dimensional case [11]:

$$\alpha_I(\mathbf{x}) = A_I(\mathbf{x}) / A(\mathbf{x}), A(\mathbf{x}) = \sum_{j=1}^N A_j(\mathbf{x}), I = \overline{1, N}. \quad (5)$$

Here N – number of natural elements for node $\mathbf{x} = (x_1, x_2)$; $A(\mathbf{x})$ – Voronoi cell area of the first order, that includes node \mathbf{x} , $A_I(\mathbf{x})$ – crossing area of Voronoi cell area of the second order \mathbf{x} with area $A(\mathbf{x})$ (refer with: Figure 1,a).

Laplace interpolation is based on neighbors defining by having the domain divided with the help of Voronoi cells [12]. Node \mathbf{x} is related to Voronoi polygon with side number equals N . Let us set polygon sides lengths by $s_I, I = \overline{1, N}$, and the heights put down from \mathbf{x} to s_I , – by h_I . Then Laplace interpolation coefficients are as follows :

$$\alpha_I = (s_I / h_I) \left(\sum_{j=1}^N s_j / h_j \right)^{-1}, I = \overline{1, N}. \quad (6)$$

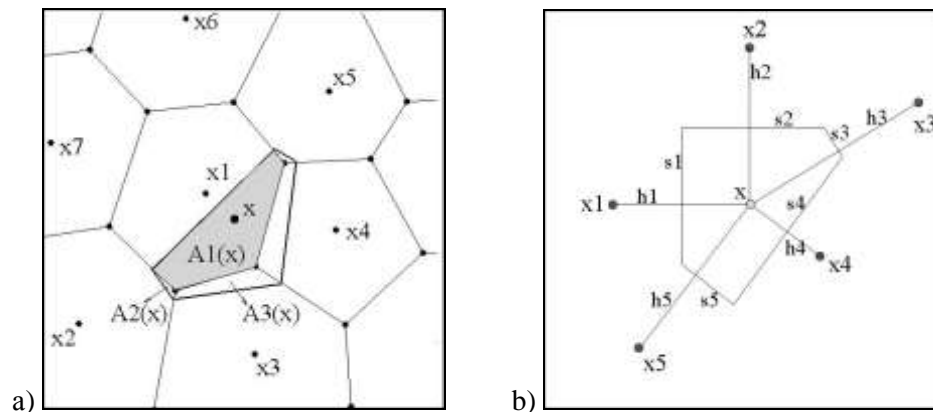


Figure 1. Interpolation by: a) Sibson; b) Laplace

This method of coefficients α_i defining is easier and cost-effective compared to Sibson's approach, as it does not require calculating polygons crossing area. Fig.1b shows Laplace interpolation architecture for two-dimensional case.

Nonsibson's interpolation has a specific feature that can be defined taking into consideration its basic properties. Many dissection polygons appear to be simplexes if the domain is divided by Voronoi cells for the specified node set. In the context of simplex polygons Laplace form functions act like linear functions. Form function behavior on some polygons is known beforehand. This fact can simplify integration problem and derivative calculation problem.

Derivative of Sibson's and Laplace's form functions can be calculated by deriving equations (5) and (6) respectively.

4. Numerical results

4.1. Solution of interaction with obstacle above the fluid surface problem

Computational domain contains reservoir with flat bottom and solid impenetrable walls filled with uniform viscous incompressible fluid and at initial time separated by thin impermeable wall that creates fluid level difference (refer with: Figure 2a). At initial time the wall starts moving upwards steadily with specified velocity while developing fluid column with zero velocity vector starts collapsing due to gravity.

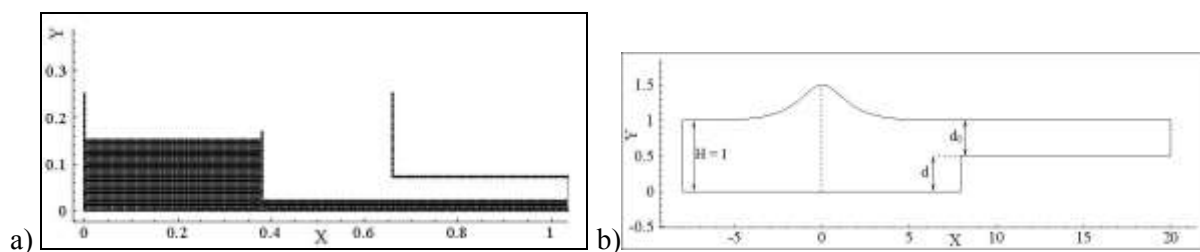


Figure 2. a) Computational domain of the problem 4.1; b) Computational domain of the problem 4.2

Peak load and maximum wave force experienced by horizontal obstacle are estimated in the context of different surface heights above free surface. Figure 3 shows flow patterns at different times for the case when height of horizontal surface quadruples layer depth. This parameter value was chosen because while dam collapsing maximum wave amplitude quadruples layer depth initial value at the bottom. It is worth noting that horizontal obstacle length was chosen in the way that moment of maximum wave amplitude coincides with the moment of wave collision with escarpment.

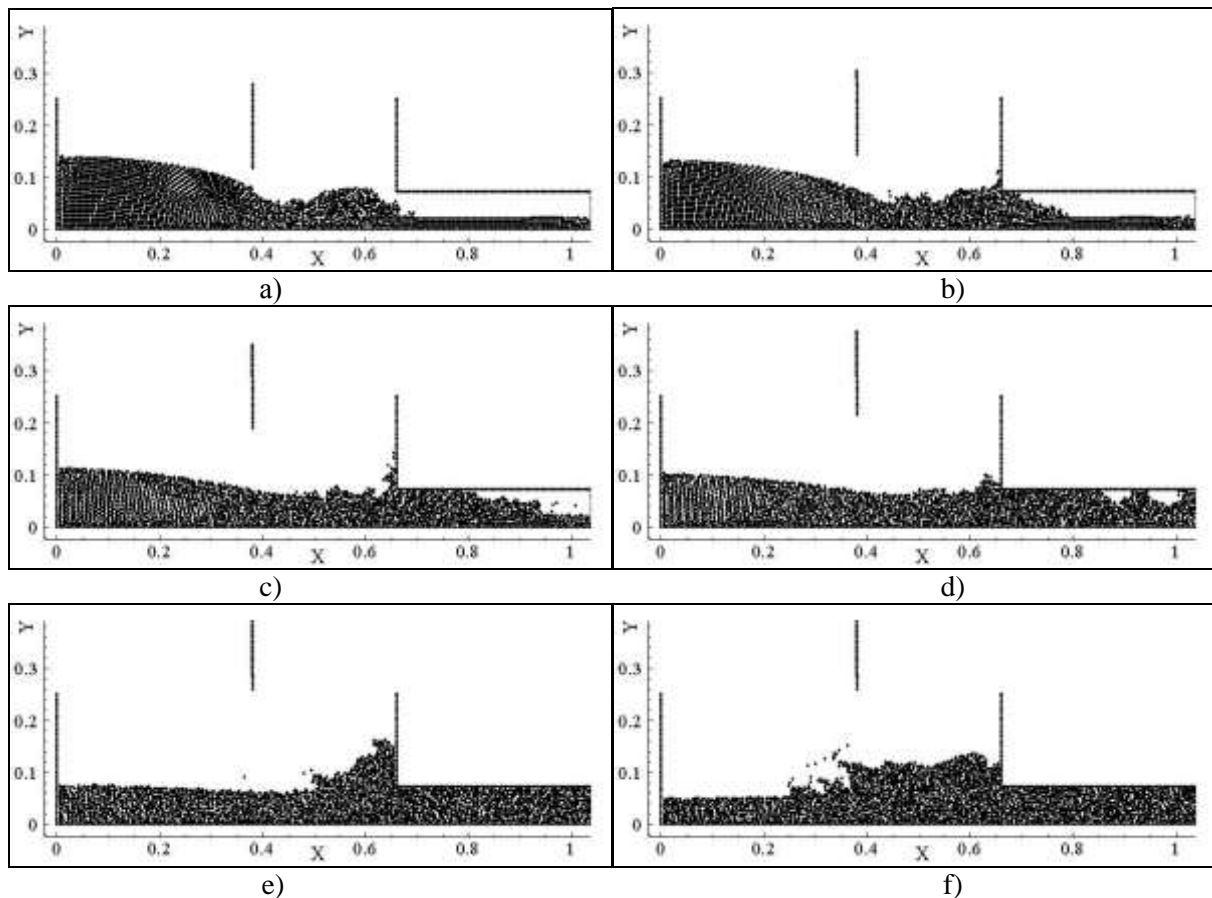


Figure 3. Interaction between the wave and the horizontal obstacle 3500 nodes (variable time step)

a) $t=0.05s$, b) $t=0.279s$, c) $t=346s$, d) $t=0.461s$, e) $t=0.694s$, f) $t=0.95s$.

The figure shows that as soon as fluid hits an obstacle it fills the escarpment in the way that waves impulses forming during motion along horizontal boundary occur until fluid reaches right wall of the reservoir. Then effect on the obstruction remains steady. It depends on flow velocity and flow vorticity.

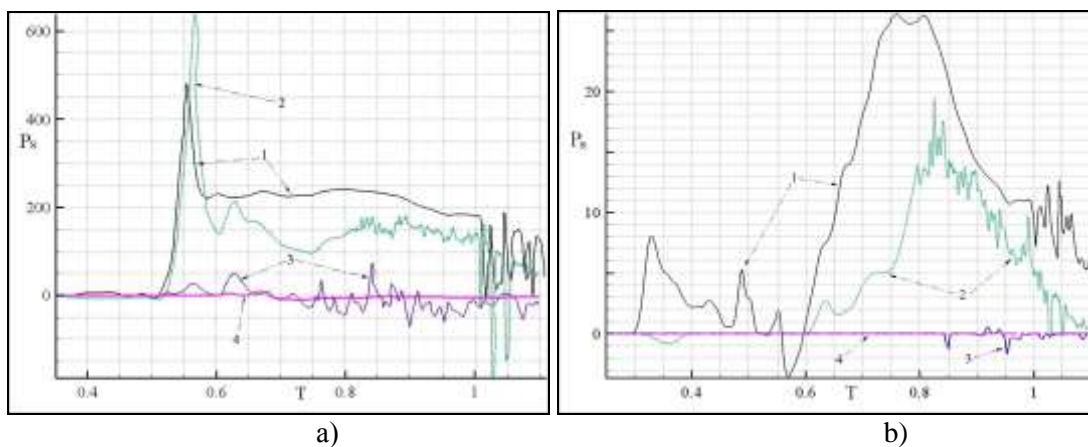


Figure 4. Chronograms of hydrodynamic load

1 – $h_g = 4h$; 2 – $h_g = 6h$; 3 – $h_g = 10h$; 4 – $h_g = 12h$

a) horizontal boundary of the escarpment; b) vertical boundary of the escarpment

In case horizontal obstacle is quite distant from free fluid surface fluid lapping at the obstacle is identified. As far as the fluid is viscous, no-slip condition is set at the solid boundary. While fluid flowing down the horizontal surface fluid particles are “released” from solid boundary and so called negative pressure zones occur at the “releasing” moment.

4.2. Solution of the problem of interaction with sledge located at the reservoir bottom

The problem was solved by using the natural elements method in the context of nondimensional variables. Figure 2b shows computational domain scheme, where d – underwater sledge height, d_0 – fluid depth above the sledge, A – arriving wave amplitude.

Figure 5 shows free surface evolution as time goes by. Wave blob occurs at the front boundary of the underwater sledge when the sledge experiences arriving wave uprush. Wave amplitude starts increasing, double bulge occurs on its surface, which later divides into reflected wave and transmitted wave. While moving along the channel transmitted wave shape transforms, the wave grows in the context of its amplitude and results in the clearly defined second wave that follows the first wave and drops behind the first wave because of the smaller amplitude and velocity. Principal waves are followed by disperse waves as well. It was mentioned in the experimental work [14].

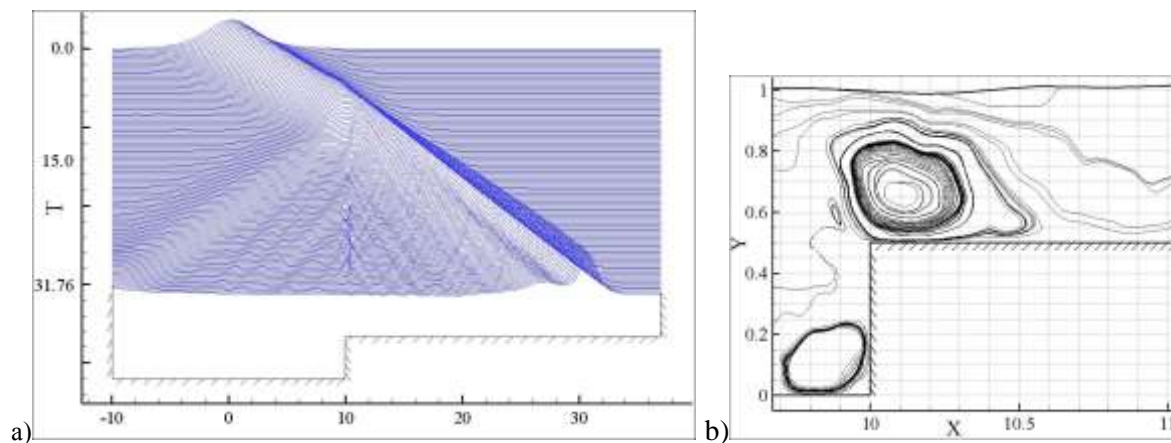


Figure 5. a) Free surface evolution; b) Vortex flows at the time $t=15.945$ s.

Table 1 shows amplitudes of transmitted waves (second and third columns) and reflected wave (forth column). The reflected wave amplitude was measured at the node with abscissa $x = 7$. The distance between the node with abscissa $x = 7$ and front boundary of the ledge equals the distance between amplitude sensor and the sledge in experiment [13]. Transmitted wave amplitude was measured at the node with abscissa $x=25$ that corresponds to last sensor location in the experiment carried out [13]. The table shows great numerical correspondence to experimental results.

Table 1. Wave amplitude

Amplitude	A_{t1}	A_{t2}	A_r
Experimental results [16]	0,2655	0,09	0,03
NEM method calculation	0,2703	0,0833	0,03036

Fig.5a shows that there is wave ripple on the surface of fluid in abscissa variation range $10 \leq x \leq 11$ (above the sledge). Vortex flow above the sledge (refer with: Figure 5b) results in wave ripple. Vortex existence is defined in experimental work [13] and in paper [14] though its impact on

transmitted waves and reflected waves is not researched yet. Small vortex of low intensity in front of front sledge boundary occurs. Figures 5,6 show flow lines while amplitude soliton wave $A = 0.1825$ moving above the sledge $d = 0.5$. Vortex velocity rotor value above the sledge is negative, that means vortex rotating direction coincides with clockwise rotation.

5. Summary

The paper presents calculation results of the problem of interaction between viscous and ideal fluid and different obstacles. The calculation results show that mesh-free method of finite elements can be considered to be applicable to solve the problems described above. It is worth mentioning the result presenting hydrodynamic loads. Load distribution diagrams are essential values to identify contractions lifetime affected by fluid and possible destroying consequences caused by wave uprushes affecting coast and bottom constructions.

The research is based on state task No 2014/64, state project “Scientific researches organization”.

References

- [1] Connor J and Brebbia K 1979 *Finite Element Techniques for Fluid Flow* (London and Boston: Newnes–Butterworth)
- [2] Patankar S V 1980 *Numerical Heat Transfer and Fluid Flow* (New York: Hemisphere Publ. Co.)
- [3] Liu G R 2003 *Mesh free methods: moving beyond the finite element method* (London: CRC Press)
- [4] Monaghan J. Smoothed particle hydrodynamics. *Ann. Rev. Astronand Astrophysics*. 1992. **No ~30**, 543–574.
- [5] Frank A M 2001 *Discrete models of incompressible fluid* (Moscow: Fizmatlit)
- [6] Facundo P. 2003 The meshless finite element method applied to a lagrangian particle formulation of fluid flows *Partial Fulfillment of the Requirements for the Degree Doctor of Philosophy. Instituto de Desarrollo tecnologico para la industria quimica (INTEC) universidad nacional del litoral noviembre* , 157 p.
- [7] Onate E and Idelsohn S.R and Zienkiewicz O C 1996 A finite point method in computational mechanics. Applications to convective transport and fluid flow *International Journal for Numerical Methods in Engineering* 39 3839
- [8] Traveroni L. Natural neighbor finite elements 1994 *In International Conference on Hydraulic Enginnering Software. Hydrosoft Proceedings 2.Computational Mechanics* Publications, pp. 291–297.
- [9] Afanasiev K E, Karabtsev S.N., Rein, T.S., Stukolov, S.V. 2011 Numerical simulation of free boundary fluid flows by using mesh–free methods *Trudy X vserossiyskogo sezda po fundamentalnym problemam teoreticheskoy I prikladnoy mekhaniki*
- [10] Skvortsov A V 2002 *Triangulyatsia Delone and its application* (Tomsk: Tomsk University)
- [11] Sibson R.. Barnett In V. (ed.) A brief description a natural neighbor interpolation *Interpret multivariate data*. – Chichester: John Wiley, (1981)pp. 21–36.
- [12] Belikov, V.V., Ivanov, V.D., Kontorovich, V.K., Korytnik, S.A., Semenov, A.U. 1997 *Nonsibson’s interpolation– new method of inetpolation of function’s values on undefined point system* 37 11
- [13] Seabra-Santos, F J and Renouard D P and Temperville A M 1987 *J. Fluid Mech.* 176 117.
- [14] Liu P. L.-F. and Y. Cheng 2001 *Physics of fluids* **13** 1660.